http://dx.doi.org/10.5012/bkcs.2012.33.8.2689

Enhancement of Photocurrent Generation by C_{60}-encapsulated Single-walled Carbon Nanotubes in Ru-sensitized Photoelectrochemical Cell

Jungwoo Lee,[a] Taehee Park, Jongtaek Lee, Mira Jang, Seungjin Lee, Heesu Kim, Sung-Hwan Han, and Whikun Yi*

Department of Chemistry and Research Institute for Natural Science, Hanyang University, Seoul 133-070, Korea
**E-mail: wkyi@hanyang.ac.kr*
Received March 9, 2012, Accepted May 14, 2012

Single-walled carbon nanotubes (SWNTs) and C_{60}-encapsulated SWNTs (C_{60}@SWNTs) are introduced to Ru-sensitized photoelectrochemical cells (PECs), and photocurrents are compared between two cells, *i.e.*, an $RuL_2(NCS)_2$/DAPV/SWNTs/ITO cell and an $RuL_2(NCS)_2$/DAPV/C_{60}@SWNTs/ITO cell. [L = 2,2'-bipyridine-4,4'-dicarboxylic acid, DAPV = di-(3-aminopropyl)-viologen, and ITO = indium-tin oxide] The photocurrents are increased by 70.6% in the presence of C_{60}@SWNTs. To explain the photocurrent increase, the reverse-field emission method is used, *i.e.*, $RuL_2(NCS)_2$/DAPV/SWNTs/ITO cell (or $RuL_2(NCS)_2$/DAPV/C_{60}@SWNTs/ITO cell) as an anode and a counter electrode Pt as a cathode in the external electric field. The improved field emission properties, *i.e.*, β (field enhancement factor) and emission currents in the reverse-field emission with C_{60}@SWNTs indicate the enhancement of the PEC electric field, which implies the improvement of the electron transfer rate along with the reduced charge recombination in the cell.

Key Words : Photocurrent, C60@SWNTs, Encapsulation, Electric field, PECs

Introduction

A typical photocurrent-generated device has photosensitizer molecules in contact with electrolytes, and these are often referred to as photoelectrochemical cells (PECs). In particular, dye-sensitized (DS) PECs are an attractive alternative to traditional solid-state photovoltaic (PV) devices (p-n junction photovoltaic devices).[1,2] In general, organic dyes possess a higher molecular excitation coefficient compared to an inorganic sensitizer, therefore, it is possible to achieve a sufficient light absorption cross-section at a reduced film thickness. Furthermore, the fabricating process for cells is much easier compared to solid-state devices. Despite these advantages, DS PECs have some serious problems such as transferring photo-generated electrons of conduction band of dye to an electrolyte solution (change recombination process).

In the past several years there has been increasing interest in methods to reduce charge recombination. One common method has been to attempt to reduce recombination by coating the thin energy barrier layer. The formation of a ZnO thin barrier layer on nanoporous TiO_2 reduced recombination and increased power conversion efficiency in PECs.[3] The other method was using single-walled carbon nanotubes (SWNTs) as a charge-collector.[4-6] SWNTs are natural electron acceptors since they act as a p-type semiconductor at ambient conditions due to adsorbed oxygen molecules in the air.[7-9] Electron transfer from nanotube to adsorbed O_2 molecules can increase hole carriers in semiconducting nanotube, thus the SWNTs significantly being able to accept electrons from materials connected to them. The low-lying end of the p* orbitals of the SWNT are very stable and readily accept electrons.[10] The 1-D structure of the SWNT closely associate with the ideal electron- or hole-transporting highway in PECs. Jang *et al*.[11] reported the covalent attachment of a ruthenium dye $[RuL_2(NCS)_2]H_2O$ (L = 2,2'-bipyridine-4,4'-dicarboxylic acid) to acid treated, shortened SWNTs by the amide bond formation using ethylenediamine as a linkage, which showed good power conversion efficiency. According to the field effective transistor data of Li *et al*.,[12] the hole density along the SWNTs was greatly enhanced in C_{60} encapsulation, which can be possibly attributed to the occurrence of electron transfer from the SWNT to C_{60} molecules. SWNTs could show higher p-type character in the case of C_{60} encapsulation inside rather than the empty SWNTs in the air.

Carbon nanotubes (CNTs) have been attractive materials in application to photovoltaic (PV) energy conversion devices,[13,14] and induced a great deal of interest in the development of new generation of organic and hybrid solar cells. Several groups reported hybrid PV devices based on a CNT/n-type Si heterojunction.[15-17] A major advantage of such an approach is the combination of charge separation at the interface of Si and CNT along with charge transport and collection. However, the role of CNT under illumination was not clear in their works. In our previous work,[12] photocurrents were compared between two cells, *i.e.*, $RuL_2(NCS)_2$/DAPV/SWNTs/ITO cell and $RuL_2(NCS)_2$/DAPV/ITO cell. [L = 2,2'-bipyridine-4,4'-dicarboxylic acid, DAPV = di-(3-aminopropyl)-viologen, SWNTs = single-walled carbon nanotubes, and ITO = indium-tin oxide] The photocurrent was raised to 83.9% in the presence of SWNTs due to the retardation of recombination reaction. Here, we introduce

[a]Present address: LG Chem. 104-1, Moonji-dong, Yuseong-gu, Daejeon 305-738, Korea

C_{60}-encapsulated SWNTs (C_{60}@SWNTs) in the above PEC, and compare the photocurrents and solar cell efficiency for the two cells, *i.e.*, one containing C_{60}@SWNTs and the other containing SWNTs. We explore the effect of C_{60}@SWNTs and SWNTs by measuring reverse-field emission (FE) currents.

Experimental

SWNTs were oxidized in a concentrated acid mixture of H_2SO_4/HNO_3 = 3:1 by volume under ultrasonication for 20-24 h at 50-60 °C, to produce shortened SWNTs with terminal carboxylic acid groups. The resulting solution was filtered by a poly(tetrafluoroethylene) membrane with a 100 nm pore size. The filtrate was washed with water by decantation to remove any remaining acid, followed by drying in an oven at 100-110 °C. Detailed process of encapsulation of C_{60} inside SWNTs (C_{60}@SWNTs) is in supplementary material S1.1. SWNTs and C_{60}@SWNTs were placed on ITO electrode by spray-coating method. DAPV (linker molecule) on SWNTs/ITO (or C_{60}@SWNTs/ITO) and successive $RuL_2(NCS)_2$ (sensitizer) on DAPV were prepared with the same method used in our previous study.[6] In order to measure photocurrent generation, the sandwich-type PEC was designed (Figure 1(a)) with [$RuL_2(NCS)_2$/DAPV/SWNTs/ITO] or [$RuL_2(NCS)_2$/DAPV/C_{60}@SWNTs/ITO)] system and Pt-sputtered ITO electrode [electrolyte: LiI of 0.1 mol/L and I_2 of 0.05 mol/L in CH_3CN].

The FE currents were measured to compare the electric field enhancement for two systems, *i.e.*, [$RuL_2(NCS)_2$/DAPV/SWNTs/ITO] and [$RuL_2(NCS)_2$/DAPV/C_{60}@SWNTs/ITO)]. Each electrode above was used as an anode and micro-texturized tip silicon (μ-tip Si) substrate was used as a cathode for the measurement of the reverse-FE currents. (See S1.2 for the preparation of textured μ-tip Si) This parallel plate diode was evacuated in a vacuum chamber at a base pressure of ~1.0×10^{-6} Torr at room temperature with a space distance to be 300 μm. A direct current voltage sweeping from 150 to 1500 V was applied to the diode sample at a step of 25 V using a Keithley 248 power supplier.

Results and Discussion

The most direct technique to prove the encapsulation of C_{60} into SWNTs is transmission electron microscopy (TEM) (see Figure S2 in the Supplementary material). Figure S2a shows the purified and unfilled SWNTs with a diameter of ~1.5 nm. Figure S2b shows the bundle of SWNTs which are filled with C_{60}. In the TEM image, the C_{60} molecules generally appear as circles with diameters of 7-8 Å sandwiched between two parallel lines corresponding to the nanotube inner wall. It is the expected and projected three-dimensional structure of C_{60}@SWNTs.

Figure 1 shows an idealized photoinduced charge transfer and energy-level arrangement of ITO, C_{60}@SWNTs, viologen and $RuL_2(NCS)_2$ (potential *vs* NHE). The lowest unoccupied molecular orbital (LUMO) of $RuL_2(NCS)_2$ is at 0.6 eV.[19,20]

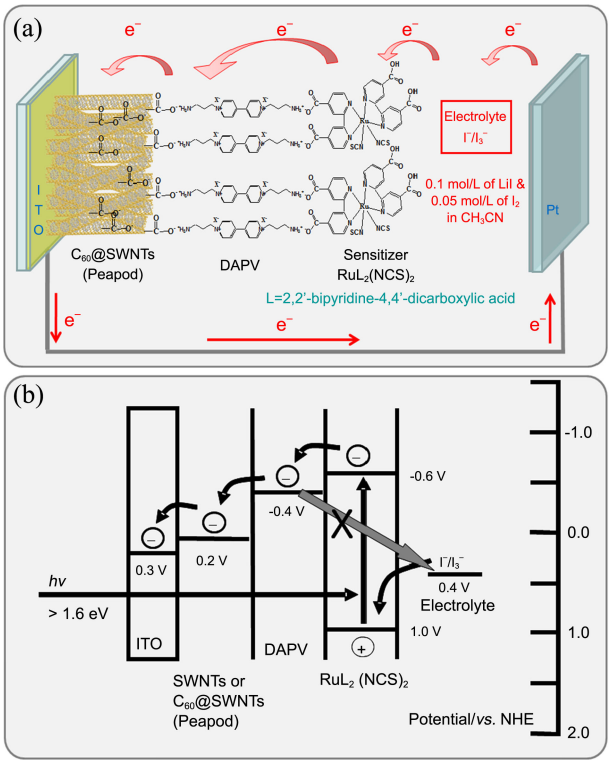

Figure 1. (a) Idealized scheme of device architectures and (b) energy-level arrangement of ITO, SWNTs, DAPV and $RuL_2(NCS)_2$ (potential/*vs*. NHE).

and Fermi level of SWNT is at 0.2 eV.[21] Generally, the gap of work function between SWNTs and C_{60}@SWNTs is thought to be small, and accepting that there is electron transfer from SWNTs to C_{60}s, then the Fermi level of C_{60}@SWNTs can be shifted to a lower direction compared to pristine SWNTs, and is estimated here at 0.1-0.2 eV. The reduction potential of viologen is 0.4 eV.[19,20] and it effectively bridges the energy gap between $RuL_2(NCS)_2$ and C_{60}@SWNTs/ITO (or SWNTs/ITO). The appropriate energy-level alignment will promote electron transfers from the LUMO of Ru-complex to the LUMO of the DAPV, C_{60}@SWNTs (or SWNTs), and ITO electrode, successively. It is expected that in the presence of C_{60}@SWNTs (or SWNTs) layer between the DAPV monolayers and ITO electrode, recombination of photoinduced electrons with oxidized sensitizer in addition to I_3^- in the electrolyte would decrease due to the energy level cascade.

As shown in Figure 2, the $RuL_2(NCS)_2$/DAPV/C_{60}@SWNTs/ITO PEC shows more outstanding photocurrent than DAPV/SWNTs/ITO PEC under illumination. The photocurrent increased immediately upon illumination and return back to its original position when the light was off. The photocurrent of the $RuL_2(NCS)_2$ on DAPV/C_{60}@SWNTs/ITO and DAPV/SWNTs/ITO showed 87 and 51 nA/cm^2, respectively. A 0 V bias was applied to the sample, when the photocurrent was measured, thus suggesting that the photocurrents originated only due to the excitations of Ru-complex sensitizer. The photocurrent was increased by 70.6% in the presence of C_{60}@SWNTs compared to pristine SWNTs.

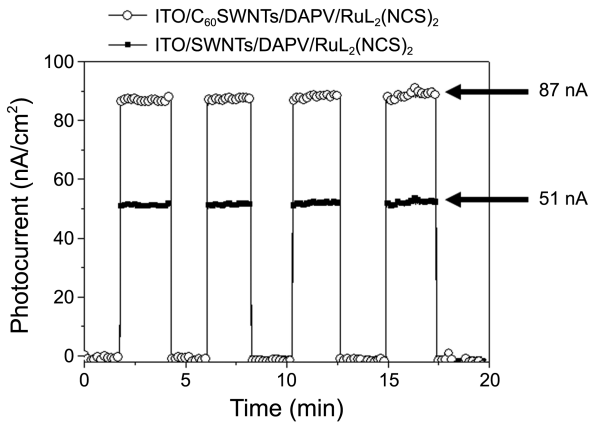

Figure 2. Photoinduced current generation of $RuL_2(NCS)_2$/DAPV/SWNTs/ITO and $RuL_2(NCS)_2$/DAPV/C_{60}@SWNTs/ITO.

Formation of $RuL_2(NCS)_2$ on DAPV/SWNTs/ITO and DAPV/C_{60}@SWNTs/ITO was also monitored by UV-vis spectra. Figure 3(a) shows the UV-vis adsorption of Ru-complexes with maximum absorption at 520 nm, which indicated good formation of $RuL_2(NCS)_2$ on DAPV/SWNTs/ITO and DAPV/C_{60}@SWNTs/ITO. The excellent formation of $RuL_2(NCS)_2$ on DAPV/SWNTs/ITO and DAPV/C_{60}@SWNTs/ITO provided a good starting point for photocurrent generation. As shown in Figure 3(b), the photocurrent spectra

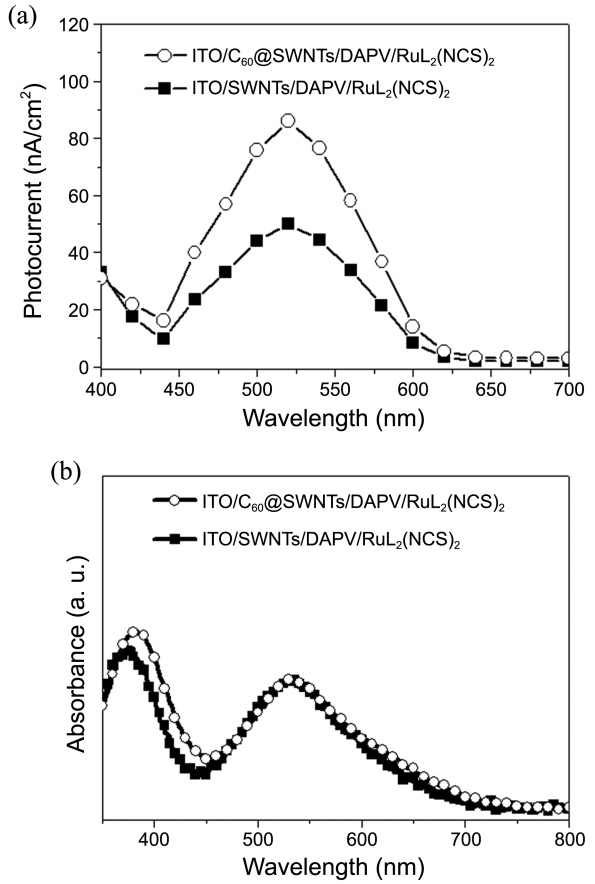

Figure 3. Action spectra of $RuL_2(NCS)_2$/DAPV/SWNTs/ITO and $RuL_2(NCS)_2$/DAPV/C_{60}@SWNTs/ITO.

followed the profile of the absorption spectrum of $RuL_2(NCS)_2$, which indicated that they were generated from the excitation of the Ru-complex. UV-Vis spectra of $RuL_2(NCS)_2$/DAPV/SWNTs/ITO and $RuL_2(NCS)_2$/DAPV/C_{60}@SWNTs/ITO were measured with the baseline of DAPV/SWNTs/ITO. The results also suggested that the recombination process was reduced further in the presence of C_{60}@SWNT layer.

With the point of energy-level arrangement, the presence of C_{60}@SWNTs seems not to be very advantageous compared with SWNTs alone. The electronic structures of C_{60}@SWNTs have been intensively studied both theoretically and experimentally. Some groups pointed out[22-24] that the intersection of the electric states of C_{60} with the Fermi level (E_F) of SWNT leads to the appearance of a multicarrier state in metallic C_{60}@SWNTs, *i.e.*, strong hybridization of electric states between C_{60} and SWNT. However, the other groups concluded[25-27] that the t_{1u} level of C_{60} inside SWNT does not lie close to the E_F, thus no structural hybridization occurred between C_{60} and SWNT. Even though many investigations have been carried out, the band structure of C_{60}@SWNTs remains a subject of controversy. Those investigations, however, affect little the energy-level arrangement of C_{60}@SWNTs or pristine SWNTs in our fabricated PECs, since their energy levels always position between the DAPV and ITO energy level with small gap difference.

In our previous studies,[6,28] the PECs containing SWNT layers showed improved efficiency of the photovoltaic devices, which was often attributed to retardation of charge recombination. The reason for the retarded recombination was suggested by three different factors. One is the formation of efficient electronic energy cascade structures.[29,30] In other words, when the conduction band of the SWNTs is placed between the work function of the ITO electrode and the conduction band of semiconductor, excited electrons can be easily transferred to the electrode through the SWNTs. The second effect of the SWNTs is the decrease of the interfacial resistance.[31,32] The electrical resistance between n-type material and ITO electrode is reduced by the outstanding conductive properties of SWNTs. The third reason is the enhancement of the electric field in the photovoltaic devices, which implies the improvement of the electron-transfer rate in the PEC.

When comparing C_{60}@SWNT layer and pristine SWNT layer, it can be said that the former has an advantage over the latter in terms of retardation of charge recombination from the results shown in Figures 2 and 3. Considering the first reason for the retardation of charge recombination, *i.e.*, efficient electronic energy cascade structures, C_{60}@SWNT layer doesn't have an advantage over the SWNT layer alone in terms of energy-level arrangement. Both energy levels transferring electrons after photon absorption seem to be located in a similar range, as mentioned previously, at cascade structures. The second effect (interstitial resistance) could not be compared directly between C_{60}@SWNTs and pristine SWNTs in our specific structured PECs [$RuL_2(NCS)_2$/DAPV/(SWNTs or C_{60}@SWNTs)/ITO]. Vavro *et al.*[33] measured the electrical resistivity for C_{60}@SWNTs and

pristine SWNTs at room temperature (300 K) and showed very small reduction of resistivity from the SWNTs to C_{60}@SWNTs, suggesting the charge transfer from C_{60} to the SWNT is minimal. On the contrary, the result of Li *et al.*[18] suggested that the hole density along the SWNT was greatly enhanced after encapsulation of C_{60}. In other words, the p-type behavior and electron acceptor property of C_{60}@SWNTs were enhanced. We estimate that increasing power conversion efficiency of PECs with C_{60}@SWNT layer would be responsible for charging collection property (more p-type character). However, that may not be sufficient to fully explain the significant improvement of photocurrents that is observed as 70.6%.

The third reason for the increase in the efficiency of photovoltaic devices by SWNTs was demonstrated by measuring electric field enhancement in In_2S_3/In_2O_3/SWNTs/ITO PEC and In_2S_3/In_2O_3/ITO PEC.[34] We explored the effect of SWNTs by measuring the reverse-field emission (FE) currents and the significant increase in the β-value (field enhancement factor) and emission currents. In general, the FE systems measuring emission currents are composed of a sample electrode as the cathode and a conductive electrode as the anode, which tend to have a relatively positive potential. However, in our case, the systems employed for investigating the effects of the SWNTs in the PEC were prepared using the layer containing SWNTs as the anode and a μ-tip Si as the cathode, which tends to have a relatively negative potential (see Figure S4 in the Supplementary material). To compare the electric field enhancement effect for pristine SWNTs and C_{60}@SWNTs, the same method, *i.e.* measuring the reverse-FE was used as shown in Figure 4. Our previous method essentially compared two photovoltaic layers, one SWNT-containing and one non-containing. SWNTs were well known as strong electron-emission materials in normal FE system, thus we could expect the strong electric field for the SWNT-containing layers since the SWNTs could be strong hole-emission materials in reverse-FE system. The reverse-FE measurement method used in Figure 4 is technically the same with the previous method, but conceptually advanced since the hole-emission ability is comparable in both SWNTs and C_{60}@SWNTs. Figure 4(a) represents the FE current densities between the anode (SWNTs/ITO and C_{60}@SWNTs/ITO) and μ-tip Si cathode. The turn-on field, E_{TO}, which was defined as the macroscopic field to produce a current density of 10 μA/cm^2, was calculated from logarithmic scale of Figure 4(a). The E_{TO} decreased from 4.42 (SWNTs anode) to 3.85 V μm^{-1} (C_{60}@SWNTs anode). The maximum FE current density was 0.21 mA cm^{-2} at an electric field of 6.2 V μm^{-1} for the PEC containing the C_{60}@SWNTs, which was 2.3 times higher than that of the PEC containing the SWNTs (0.09 mA cm^{-2}). The FE current was increased and E_{TO} value was decreased in the presence of C_{60}@SWNT layer.

Materials in a strong applied electric field, E = *V*/d (*V*: applied electric potential, d: inter distance between an anode and a cathode), emit electrons by tunneling according to the following Flower-Nordheim (F-N) equation,[35,36]

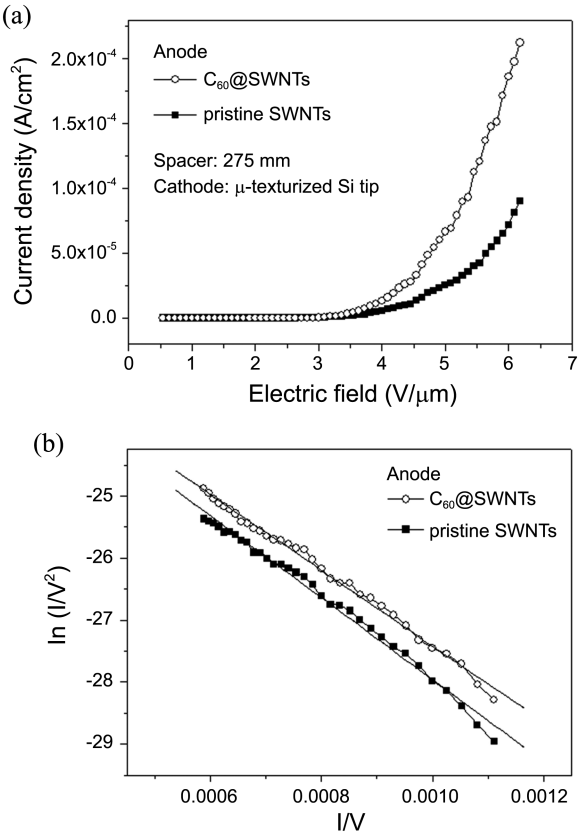

Figure 4. (a) reverse-FE current densities and (b) F-N plots for the anode of $RuL_2(NCS)_2$/DAPV/SWNTs/ITO and $RuL_2(NCS)_2$/DAPV/C_{60}@SWNTs/ITO.

$$I = AV^2 \exp\left(-\frac{b\Phi^{3/2}}{\beta V}\right).$$

where *I* is the FE current density, *A* and *b* are constants, Φ is the work function, and β is the geometric enhancement factor, *i.e.*, the field enhancement factor. Figure 4(b) shows the F-N plots obtained from the FE data in Figure 4(a). The β-values of SWNTs and C_{60}@SWNTs on the ITO anode were calculated by the F-N equation and were found to be 3001 and 3615, respectively, showing ~20% increase. In this study, the geometrical feature of these two samples with the μ-tip Si cathode was not significantly changed. The only difference is the existence of the SWNT or C_{60}@SWNT layer in the anode electrode. In general, the measurements of the FE currents and FE characteristics are influenced by the work function and geometry of the cathode tip. However, in this present study, the cathode materials used for the FE measurements were the same. These results imply that the C_{60}@SWNT layer lead to increase in the FE currents over the SWNT layer due to the enhanced electric field around the μ-tip Si cathode. From the point of view of the field of photovoltaic devices, the enhanced electric field intensifies the power of electron transfer, which leads to the improvement of the electron-transfer rate in the cell. The PECs used in this study are different from semiconducting p-n junction devices having depletion layer with internal voltage differ-

ence inside. However, the generated electrons and holes transfer to lower energy levels successively after absorbing photons, in other words, they are in electric field (E = V/d) before reaching electrodes. To elucidate the charge carrier mobility, life time of the carriers, electric field change, *etc*, in our PECs, a technique of photoinduced charge carrier extraction in a linearly increasing voltage (Photo-CELIV)[37] is necessary and under investigation.

The photocurrent increase with the SWNTs was explained in our previous studies,[6,28,30] *i.e.*, the formation of an efficient electronic energy cascade structure, decreasing the interfacial resistance, and improving the electrical field. The further improvement with C_{60}@SWNTs was due to the increased electron acceptor property and the enhanced electric field after the encapsulation of C_{60} inside SWNTs.

Conclusion

In conclusion, we have compared photocurrents for $RuL_2(NCS)_2$/DAPV/SWNTs/ITO PEC and $RuL_2(NCS)_2$/DAPV/C_{60}@SWNTs/ITO PEC under illumination of light. The photocurrents and efficiency were increased 70.6% in the presence of C_{60}@SWNTs. The improved field emission properties, *i.e.*, β and emission currents in the reverse-FE with C_{60}@SWNTs indicated the enhancement of electric field in the PEC, which implied the improvement of the electron transfer rate along with the reduced charge recombination in the cell. These results suggested that C_{60}@SWNTs can improve the efficiency instead of SWNTs in optoelectronic devices.

Acknowledgments. This study was supported by the National Research Foundation of Korea funded by the Ministry of Education, Science, and Technology (2011-0028850, 2011-0027329, and 2011-0003056).

References

1. Kim, Y. G.; Walker, J.; Samuelson, L. A.; Kumar, J. *Nano Lett.* **2003**, *2*(4), 523.
2. Hara, K.; Sayama, K.; Ohga, Y.; Shinpo, A.; Suga, S.; Arakawa, H. *Chem. Commun*. **2001**, *6*, 569.
3. Mane, R. S.; Lee, W. J.; Pathan, W. J.; Han, S. H. *J. Phys. Chem. B* **2005**, *109*(51), 24254.
4. Sheeney-Haj-Ichia, L.; Basnar, B.; Willner, I. *Angew. Chem. Int. Ed*. **2004**, *44*(1), 78.
5. Lee, T. Y.; Alegaonkar, P. S.; Yoo, J. B. *Thin Solid Films* **2007**, *515*(12), 5131.
6. Robel, I.; Bunker, B. A.; Kamat, P. V. *Adv. Mater*. **2005**, *17*(21), 2458.
7. Sumanasekera, G. U.; Adu, C. K. W.; Fang, S.; Eklund, P. C. *Phys. Rev. Lett*. **2000**, *85*(5), 1096.
8. Bradley, K.; Jhi, S. H.; Hone, P. G.; Hone, J.; Cohen, M. L.; Louie, S. G.; Zettl, A. *Phys. Rev. Lett*. **2000**, *85*(20), 4361.
9. Collins, P. G.; Bradley, K.; Ishigami, M.; Zettl, A. *Science* **2000**, *287*, 1801.
10. Li, J. Q.; Zhang, Y. F.; Zhang, M. X. *Chem. Phys. Lett*. **2002**, *364*, 328.
11. Jang, S. R.; Vittal, R.; Kim, K. J. *Langmuir* **2004**, *20*(22), 9807.
12. Li, Y. F.; Kaneko, T.; Hatakeyama, R. *Appl. Phys. Lett*. **2008**, *92*(18), 183115.
13. Lee, J. U. *Appl. Phys. Lett*. **2005**, *87*(7), 073101.
14. Ong, P. L.; Euler, W. B.; Levissky, I. A. *Nano Technol*. **2010**, *21*(10), 105203.
15. Wei, J.; Jia, Y.; Shu, Q.; Gu, Z.; Wang, K.; Zhuang, D.; Zhang, G.; Wang, Z.; Luo, J.; Cao, A.; Wu, D. *Nano Lett.* **2007**, *7*, 2317.
16. Tzolov, M. B.; Kuo, T. F.; Straus, D. A.; Yin, A.; Xu, J. J. *J. Phys. Chem. C* **2007**, *111*(15), 5800.
17. Li, Z.; Vasyl, P. K.; Viney, S.; Xu, Y.; Dervishi, E.; Salamo, G. J.; Biris, A. R.; Biris, A. S. *Appl. Phys. Lett.* **2008**, *93*(24), 243117.
18. Lee, W. J.; Lee, J. W.; Lee, S. H.; Chang, J. H.; Yi, W. K.; Han, S. H. *J. Phys. Chem. C* **2007**, *111*(26), 9110.
19. Hyung, K. H.; Kim, D. Y.; Han, S. H. *New J. Chem*. **2005**, *29*(8), 1022.
20. Lee, W. J.; Hyung, K. H.; Kim, Y. H.; Cai, G.; Han, S. H. *Electrochem. Commun*. **2007**, *9*, 729.
21. Bhattacharyya, S.; Kymakis, E.; Amaratunga, G. A. J. *J. Chem. Mater*. **2004**, *16*(23), 4819.
22. Okada, S.; Otani, M.; Oshiyama, A. *Phys. Rev. B* **2003**, *67*(20), 205411.
23. Okada, S.; Otani, M.; Oshiyama, A. *Phys. Rev. B* **2003**, *68*(12), 125424.
24. Hombaker, D. J.; Kahng, S. J.; Misra, S. B.; Smith, B. W.; Johnson, A. T.; Mele, E. J.; Luzzi, D. E.; Yazdani, A. *Science* **2002**, *295*, 828.
25. Dubay, O.; Kresse, G. *Phys. Rev. B* **2004**, *70*(16), 165424.
26. Pichler, T.; Kukovecz, A.; Kuzmany, H.; Achiba, H. Y. *Phys. Rev. B* **2003**, *67*(12), 125416.
27. Shiozawa, H.; Ishii, H.; Kihara, H.; Sasaki, N.; Nakamura, S.; Yoshida, T.; Takayama, Y.; Miyahara, T.; Suzuki, S.; Achiba, Y.; Kodama, T.; Higashiguchi, M.; Chi, X. Y.; Nakatake, M.; Shimada, K.; Namatame, H.; Taniguchi, M.; Kataura, H. *Phys. Rev. B* **2006**, *73*(7), 075406.
28. Lee, W. J.; Lee, J. W.; Yi, W. K.; Han, S. H. *Adv. Mater.* **2010**, *22*(20), 2264.
29. Kymakis, E.; Amaratunga, G. A. J. *Sol. Energy Mater. Sol. Cells* **2003**, *80*(4), 465.
30. Lee, W. J.; Lee, J. W.; Yi, W. K.; Han, S. H. *Appl. Phys. Lett*. **2008**, *92*(15), 153510.
31. Arranz-Andres, J.; Blau, W. J. *Carbon* **2008**, *46*(15), 2067.
32. Lee, K. M.; Hu, C. W.; Chen, H. W.; Ho, K. C. *Sol. Energy Mater. Sol. Cells* **2008**, *92*(12), 1628.
33. Vavro, J.; Llaguno, M. C.; Satishkumar, B. C.; Luzzi, D. E.; Fischer, J. E. *Appl. Phys. Lett*. **2002**, *80*(8), 1450.
34. Lee, J. W.; Lee, W. J.; Park, E. K.; Park, T. H.; Nah, Y. C.; Han, S. H.; Yi, W. K. *Appl. Phys. Lett*. **2010**, *96*(17), 173506.
35. Lee, J. W.; Lee, W. J.; Sim, K. J.; Han, S. H.; Yi, W. K. *J. Vac. Sci. Technol. B* **2008**, *26*(2), 847.
36. Lee, J. W.; Lee, W. J.; Sim, K. J.; Han, S. H.; Yi, W. K. *J. Vac. Sci. Technol. B* **2008**, *26*(6), 1892.
37. Mozer, A. J.; Sariciftci, N. S.; Lutsen, L.; Vanderzande, D. Osterbacka, R.; Westerling, M.; Guska, G. *Appl. Phys. Lett.* **2005**, *86*, 112104.